受入
91-8-520
高工研図書室

CERN-TH.6096/91
ISN 91.45

# THE ORIGIN OF P-WAVE ENHANCEMENT IN THE OPTICAL MODEL FOR LOW ENERGY PROTON-ANTIPROTON SCATTERING

J. Carbonell[1)], O.D. Dalkarov[2)], K.V. Protasov[2)], and I.S. Shapiro[2,3)]

*1) Institut des Sciences Nucléaires, 53 Ave. des Martyrs, F-38026 Grenoble*
*2) Lebedev Physical Institute, Leninsky pr., 53, 117924 Moscow, USSR*
*3) Theoretical Physics Division, CERN, CH-1211 Geneva 23, Switzerland*

## ABSTRACT

The observed large P-wave contribution to the $\bar{N}N$ interaction at low energies, reproduced by the optical model calculations, is shown to be caused by the S-matrix poles which correspond to the P-wave states located close to the $\bar{N}N$ threshold.

CERN-TH.6096/91

May 1991

## 1. INTRODUCTION

One of the impressive results obtained in the experiments with antiproton ( $\bar{p}$) beams in the Low Energy Antiproton Ring (LEAR) is the abnormally large P-wave (relative orbital momentum of proton and antiproton L = 1) contribution to different observables: the $\bar{p}p$ elastic scattering [1] ($\sigma_e$), the charge-exchange reaction ( $\bar{p}p \rightarrow \bar{n}n$) [2] ($\sigma_{ce}$), the annihilation cross-section ($\sigma_a$), the P-states widths of the $\bar{p}p$ atom (protonium) [3], and the real-to-imaginary ratio ($\rho$ parameter) for the forward elastic $\bar{p}p$ scattering amplitude [4] at very low centre-of-mass momenta, k, of the colliding particles (k < 150 MeV/c). Moreover, it was observed that the P-wave contribution even grows with k decreasing from 150 to 100 MeV/c (see [5] and references therein).

On the other hand, the canonical theoretical treatement predicts a quite opposite k-dependence of the partial wave cross section at low momentum k. Due to centrifugal repulsion, it is expected that at kR < L (R is the effective $\bar{N}N$ nuclear interaction range) the behaviour of the partial cross sections should be

$$\sigma_{e,ce} = 4\pi\ |C_{e,ce}^{(L)}|^2\ \chi_L^{\,4}(kR) \tag{1}$$

$$v\sigma_a = 4\pi\ |C_a^{(L)}|^2\ \chi_L^{\,2}(kR) \tag{2}$$

where

$$\chi_L(kR) = \frac{(kR)^L}{[(2L+1)!!]}\,. \tag{3}$$

Here v = 2k/M denotes the relative velocity of $\bar{p}$ and p, and M is the nucleon mass. The quantities $C^{(L)}$ are smooth functions of k and L, so that $|C^{(L)}|$ can be approximately considered as constants, equal to R in order of magnitude.

Therefore, according to eqs. (1-3), the P-wave contributions to the cross sections should be ten times less than those from the S-wave ones even at $k \sim R^{-1}$. But the analysis of the experimental data shows that S and P partial amplitudes are

comparable [1]. This means that values of $|C^{(L)}|$ are very large and they compensate for the smallness of centrifugal factors defined by $\chi_L$.

A natural physical reason for the enhancement of the P-wave amplitudes in low energy $\bar{p}p$ collisions is the possible existence of the near-threshold (close to 2M) quasinuclear bound or resonant $\bar{N}N$ P-states. These states should appear because of the strongly attractive nuclear forces between $\bar{N}$ and N. The corresponding poles of the $\bar{p}p$ scattering amplitude would then naturally lead to P-wave enhancement. This fact was first emphasized qualitatively in reference [6], a long time before appearance of the sophisticated experimental data.

The main problem of the quantitative theory is making the right choice when taking into account the annihilation of the $\bar{N}N$ pair. The first choice historically used was the optical model (OM) in which the strong absorption caused by annihilation is described by means of a non- Hermitian Hamiltonian [7].

Another possible approach is a unitary coupled-channels model (CCM). In the latter, both $\bar{N}N$ and the annihilation (two-meson) channels are introduced explicitly and considered coupled with each other by some Hermitian interaction Hamiltonian.

The most important difference between OM and CCM comes from the fact that in the CCM case not only the annihilation ( $\bar{N}N \rightarrow$ mesons) but also the inverse "reannihilation" process (mesons $\rightarrow \bar{N}N$) are taken into account and automatically included in the calculations. A direct consequence of that is the fact that in the CCM, the annihilation widths of quasinuclear levels are substantially reduced compared to those given by OM (see, for instance, reference [8]).

The calculations performed within the framework of the CCM with realistic $\bar{N}N$ nuclear forces (OBEP) reproduce quite well all experimental data on low energy $\bar{p}p$ interactions [5], [9], [10], [11]. In these papers the quasinuclear P-levels responsible for the P-wave enhancement were evaluated and their widths were shown to be of the order of normal hadron size (from few tens to one hundred MeV).

It seemed that these CCM results definitely explain the physical nature of the observed large P-wave contribution to the $\bar{p}p$ low energy interaction.

At the same time a satisfactory description of the experimental data under consideration was obtained in the OM calculations [12], [13], [14]. Despite the fact that the widths of the $\bar{N}N$ levels given by OM are usually larger than those in CCM, one cannot exclude that in some variants of the OM fitting the experimental data, there are one or few near-threshold P-states giving the observed P-wave enhancement. This possibility should be confirmed by direct calculations. Otherwise the conclusion that bound and resonant states manifest themselves in the phenomena discussed above would be model-dependent and so questionable.

An attempt at such an analysis was made by Lacombe et al. in reference [14]. In this paper the Argand diagrams of the partial scattering amplitudes were studied. At least one of them ($^{13}P_0$) was found to have resonance-like structure (see Figure 1). It was also demonstrated that this amplitude could be approximated by a sum of Breit-Wigner-like resonant amplitude plus a smooth term originating from singularities located far from the threshold. The best fit gave the following positions, ($E_0$), and widths, ($\Gamma$), of the near-threshold $^{13}P_0$ level: $E_0$ = - 1.91 MeV, $\Gamma$ = 10.6 MeV and $E_0$ = - 0.2 MeV, $\Gamma$ = 10.2 MeV for the Paris and Dover-Richard potentials respectively.

This result indicates that in OM the P-wave enhancement may also be connected with the existence of near-threshold P-levels in the $\bar{N}N$ system. In addition it points out that these levels, being located extremely close to the threshold, can be narrow.

Nevertheless, these conclusions, following from reference [14], need to be confirmed in two aspects. Firstly, the singular terms in the partial scattering amplitudes, being supposed to exist *a priori*, were introduced "by hand" into the fitting procedure. Thus, it seems necessary to evaluate such levels directly by solving the eigenvalue problem for the non-Hermitian OM Hamiltonian. Secondly, it

is necessary to check the existence of the $\bar{N}N$ near-threshold P-levels in OM versions which are different from those considered in reference [14], but also describing the bulk of the low energy $\bar{p}p$ experimental data and particularly the large P-wave contribution to the cross sections.

The aim of this paper is to examine these two questions. As the corresponding numerical calculations are cumbersome it is necessary to make a reasonable choice for the OM version to study. We have chosen the optical potential proposed by M. Kohno and W. Weise (KW) [13]. This potential differs substantially from the Paris potential. For instance, the absorption range (i.e. the radius of the imaginary part of the optical potential) in the KW model is twice as large as in the Paris potential. At the same time the KW potential fits satisfactorily all the considered experimental data. It is remarkable that the energy dependence of some P-wave partial amplitudes is very similar for different OM (see Figure 1).

Nevertheless, an attempt was made in Reference [13] to explain the large contribution of P-waves as a result of suppression in the S-wave $\bar{p}p$ partial scattering amplitudes rather than P-wave enhancement. This statement is difficult to understand because the scattering lengths in the KW model are normal (of the order of 1 fm). Neglecting Coulomb effects and the n-p mass difference we have obtained the following $\bar{p}p$ scattering lengths: $a_{\bar{p}p}(^1S_0) = 0.52 - 0.98i$ fm and $a_{\bar{p}p}(^3SD_1) = 1.00 - 0.79i$ fm, in agreement with the experimental data from protonium shifts and widths [3].

These reasons pushed us to make a direct search of poles in the complex momentum plane of the P-wave partial $\bar{p}p$ scattering amplitudes in the KW version of the OM.

The plan of the paper is the following. In Section 2 we analyse the energy behaviour of P-wave scattering amplitudes in the KW potential, which we have calculated. Section 3 is devoted to a general description of some analytical properties of the amplitudes for Hermitian and non-Hermitian interaction Hamiltonians.

Section 4 contains the results of numerical calculations of the eigenvalues and resonances in the KW potential. In Section 5 some remarks on the difference between the OM and the CCM wave functions inside the interaction region are discussed and a general conclusion is presented.

## 2. ENERGY DEPENDENCE OF THE PARTIAL WAVE CROSS SECTIONS

In the KW model, $\bar{N}N$ interaction is described by a complex, local, and energy-independent potential which will be written in the following way:

$$V_{\bar{N}N}(r) = V_{OBEP}(r) + iW(r) \tag{4}$$

Here, $V_{OBEP}$ is the G-parity transform of the NN Ueda potential [15] regularised below some cut-off radius $r_c$. This cut-off is needed to avoid the singular terms in OBEP caused by spin-orbit and tensor forces.

W is the imaginary part of the KW potential for taking into account the annihilation. It has the usual Woods-Saxon form:

$$W(r) = -\frac{W_0}{1 + e^{\frac{r - R_0}{a}}}. \tag{5}$$

The model has four parameters ($r_c$, $W_0$, $R_0$, a) which were fixed by fitting the experimental data: $r_c$ = 1 fm, $W_0$ = 1.2 GeV, $R_0$ = 0.55 fm, a = 0.2 fm. However, for a better understanding of this model we will vary the parameters $W_0$ and $r_c$.

We have calculated the different partial P-waves elastic ($\sigma_e$) and annihilation ($\sigma_a$) cross sections. In order to investigate their relative contributions to the total cross sections, we remove from them, following equations (1)-(3), the trivial kinematical and statistical factors by introducing the reduced elastic ($\bar{\sigma}_e$) and annihilation ($\bar{\sigma}_a$) cross sections:

$$\bar{\sigma}_e = \frac{\sigma_e(k)}{(2J+1)\pi k^4}, \tag{6}$$

$$\bar{\sigma}_a = \frac{\sigma_a(k)}{(2J+1)\pi k}. \tag{7}$$

These reduced cross sections are proportional to the squared modulus of the functions $C^{(L)}(k)$ in equations (1)-(3).

Results for all P partial waves are presented in figures 2a and 2b. They correspond respectively to isospin T = 0 and T = 1 states in the standard spectroscopic convention $^{2T+1,2S+1}L_J$. Results corresponding to a "pure annihilation scattering", i.e. obtained by putting $V_{OBEP} = 0$ in equation (4), are also included.

We remark, from a global comparison between Figures 2a and 2b, that the $\bar{N}N$ P-wave scattering is dominated by T = 0 channels. The reduced cross sections are greater in T = 0 states, roughly speaking by a factor 10, than the vertical scaling factor used in the Figure 2b plot.

Another conclusion which can be drawn from this figure is that the large P-wave contribution in the optical model is not produced by annihilation, but is generated by nuclear forces. Indeed, annihilation scattering ($V_{OBEP}=0$ curves in Figures 2a and 2b) is two orders of magnitude out.

From Figures 2 we also see that the most important P-wave is $^{13}P_0$. Its anomalously big contribution was already noticed in [16], where the protonium level shifts and widths in the KW potential were calculated.

The same feature is even more clearly seen in the reduced $\bar{p}p$ annihilation cross sections $\bar{\sigma}_a(k)$ shown in Figure 3. We see that all reduced cross sections are practically constant in the k-region from 0 to 100 MeV/c and that the anomalously big value of the $^{13}P_0$ cross section is also accompanied by the strongest energy dependence.

These facts, the big value and the strong energy dependence in the $^{13}P_0$ amplitude suggest the existence of near-threshold singularities. The next sections will be devoted to the demonstration that this is really the case.

## 3. S-MATRIX SINGULARITIES IN THE OPTICAL MODELS

Before going into details of the considered particular potential we will discuss some general features of isolated singularities of the amplitude that can be found in any optical model.

Let us introduce the Jost function, $a_\alpha(W_0,k)$, by writing the reduced regular radial solution of the Schrödinger equation, $u_\alpha$, in the asymptotic region as

$$u_\alpha(W_0,k,r) = \frac{1}{2ik}\left(a_\alpha(W_0,-k)\ e^{ikr} - a_\alpha(W_0,k)\ e^{-ikr}\right) \tag{8}$$

where $W_0$ is the "annihilation strength" introduced in (5) and $\alpha = (S,L,J,T)$ labels the set of the quantum numbers of the state (i.e. spin, orbital and total angular momentum, and isospin respectively).

The S matrix is then given by the formulas:

$$S = (-)^L \frac{a(W_0,-k)}{a(W_0,k)} = (-)^L \frac{a^*(-W_0,k^*)}{a^*(-W_0,-k^*)}. \tag{9}$$

To obtain the latter equality we used the symmetry relation:

$$a(W_0,k) = a^*(-W_0,-k^*) \tag{10}$$

Let us emphasize here the difference between this symmetry relation (10) and the corresponding one in the case of the two coupled-channels model. In the latter case, the relation is the same as for a Hermitian potential problem, i.e. $a(k) = a^*(-k^*)$,

despite the fact that annihilation is taken into account. This question was discussed in detail in [17] (see also references therein).

In Figure 4 we present the complex momentum plane (K) and the two so-called physical ($E_I$) and unphysical ($E_{II}$) energy sheets of the Riemannian energy manifold into which it is mapped. The K plane is divided into eight sectors (I—VIII) and the E-sheets into the corresponding quadrants. We use the following notations:

$$k = k_1 + ik_2, \tag{11}$$

$$E = \frac{k^2}{M} = \frac{(k_1^2 - k_2^2) + 2ik_1k_2}{M}, \tag{12}$$

M is the nucleon mass.

The poles of the S-matrix are given by isolated zeros of the Jost function in the K-plane and they correspond to bound (Im k > 0) or resonant states (Im k < 0).

In the Hermitian case, bound states are restricted to the positive K-imaginary axis or the negative real axis on the physical energy sheet $E_I$ ($B_0$ in Figure 4). Resonances appear in the lower half K-plane by pairs ($k_0$, $-k_0^*$) which are symmetric with respect to the imaginary axis ($R_0$ and $R_0'$ in Fig. 4) according to relation (10) if $W_0 = 0$. In this case the symmetry relation (10) allows us to write the S-matrix for the momentum k in the form

$$S(k) = \bar{S}(k)\,\frac{(k + k_0)(k - k_0^*)}{(k - k_0)(k + k_0^*)}, \tag{13}$$

where the unimodular factor $\bar{S}(k)$ does not contain the poles $k_0$ and $-k_0^*$. This expression leads to the usual resonant Breit-Wigner form for scattering cross section:

$$\sigma(k) \sim \frac{1}{(E - E_0)^2 + \frac{\Gamma^2}{4}} \tag{14}$$

with the position $E_0$ and width $\Gamma$ of the resonance given by the equalities

$$E_0 = |k_0|^2/M \qquad \Gamma(k) = -4\ \mathrm{Im}(k_0)\ k/M. \tag{15}$$

In the case of sharp resonance the width is usually defined as $\Gamma_0 = \Gamma(|k_0|)$. Starting from this picture, we will switch on the annihilation potential step by step and follow the different kinds of pole trajectories ($\gamma$) which can be expected from general principles.

Let us begin by considering the trajectory of a pole which in the Hermitian case was a bound state. There are two possible cases. The first one is represented by trajectory $\gamma_1$ up to $B_1$ in Fig. 4. This pole moves apart from the imaginary axis but remains in sector III. In this situation the physical interpretation of this pole as an unstable bound state is possible. The total mass of the system is smaller than 2M; the decay into $\bar{N}N$ is thus forbidden and the $\bar{N}N$ wave function tends exponentially to zero when $r \to \infty$.

The second case appears when the pole trajectory moves up to $B_2$, crossing the bisector separating regions III and IV. In that case the possibility of any physical interpretation of such a state is lost. The total mass of the system becomes greater than 2M but the decay into $\bar{N}N$ is still impossible because according to (8) the wave function of such a state decreases exponentially at large r.

Let us discuss now the possible trajectories of states which in the Hermitian case are associated with resonances (points $R_0$ and $R_0'$ in Fig. 4). When we switch on the annihilation we immediately lose the symmetry of these poles, which directly follows from property (10) for the complex potential. The right pole $R_0$ follows a trajectory $\gamma_3$ up to some point $R_1$ which will be located in the quadrant VII (Re E < 0) or VIII (Re E < 0) depending on the strength of the annihilation potential. The left $R_0'$ pole, in the case of small influence of annihilation, has a trajectory $\gamma_3'$ up to

some point $R_1'$, but for strong annihilation it crosses the K real axis and reaches the point $R_2'$ in sector IV (Im k > 0).

As was pointed out above, the poles lying in sector IV do not correspond to any physical state of the $\bar{N}N$ system. The existence of these singularities was discussed in connection with the problem of $\Sigma$-nuclear states in references [18,19]. It should be mentioned that a "mirror" pole R' in sector V never defines a physical state by itself. Even in the Hermitian case the corresponding energy $k'_0{}^2/M$ has a positive imaginary part, leading to an exponentially- increasing time-dependent solution of the Schrödinger equation which is physically senseless.

As follows from equations (13) and (14), the pair of poles ($R_0$, $R_0'$) is needed to obtain a resonance behaviour of the amplitudes whether the symmetry is exact, as in the Hermitian case, or approximate, as for some states in optical models.

We have presented the possible pole trajectories in a complex potential. As will be shown in the following Section, the discussed possibilities are realized in the KW model. The most non-trivial fact will be the existence of narrow near-threshold $\bar{N}N$ quasinuclear states in an optical model even with relatively large annihilation range.

## 4. QUANTITATIVE RESULTS ON BOUND AND RESONANT $\bar{N}N$ STATES IN KW MODEL

The strong attractive $\bar{N}N$ OBEP interaction creates a rich spectrum of bound and resonant states and their properties have been widely studied by many authors (see Refs. [14,20,21]). Two papers [14,21] have been devoted to the study of some of these singularities and their influence on the scattering observables when the annihilation is included . We will present in this section numerical results for all bound and near-threshold resonant states in the KW optical model for S and P partial waves.

The method we used is based on a computation of the Hamiltonian, H, and inverse Green function, $G^{-1}(k)$, in a configuration space lattice, i.e.:

$$H_{m,n} = \langle x_n|H|x_m\rangle \tag{16}$$

$$G^{-1}(k)_{m,n} = k^2\delta_{m,n} - H_{m,n} + i\varepsilon \tag{17}$$

Bound and resonant states are then obtained in a uniform way by looking at the complex zeros of the determinant $\Delta(k) = \det[G^{-1}(k)]$ in the K-plane. This procedure, which is numerically non-trivial, allows a direct calculation of singularities without any additional fitting procedure of the scattering amplitudes.

### Bound states

In Figure 5 we have plotted the S and P bound-state trajectories in the KW potential, parametrized by the annihilation strength $W_0$. As could be expected, the most attractive interactions are found in the T = 0, S = 1 channels. For these quantum numbers the contribution to OBEP forces from all mesons add coherently, resulting in a very strong potential [20]. For instance $^{13}SD_1$ and $^{13}P_0$ ground states have binding energies greater than 1 GeV, values which are unacceptable in any believable non-relativistic approach.

The majority of trajectories lie entirely in the physical sector III. However the less bound states move into region IV, appearing as "positive energy bound states", i.e. with total mass greater than 2M and, as discussed in the previous paragraph, without any physical meaning. Their overall evolution is shown in Figure 6, where concrete examples of a $\gamma_1$-like trajectory in the K-plane are plotted for the partial waves $^{11}S_0$, $^{31}S_0$, and $^{31}SD_1$.

It is also interesting to notice from Figure 5a a common property of all trajectories remaining in sector III. They move parallel to each other and obtain practically the same imaginary part for $W_0 = 1200$ MeV. This can be understood from the integral expression for the width of a state:

$$\frac{\Gamma}{2} = - \int_0^\infty \left| \Psi_\alpha(r) \right|^2 W(r) r^2 dr , \tag{18}$$

Assuming the state to be deep enough and localized inside a region with practically constant imaginary potential, we obtain from equation (18):

$$\frac{\Gamma}{2} \sim - W(0) \int_0^\infty \left| \Psi_\alpha(r) \right|^2 r^2 dr \tag{19}$$

For normalized wave functions, the integral in the latter equality is, of course, independent of the state's quantum numbers.

From the physical point of view, the behaviour of the width as a function of the binding energy of the state should be different. Roughly speaking, the width is expected to be proportional to the phase volume of the mesons in the final (i.e. annihilation) channel. With increasing binding energy (i.e. decreasing effective mass) of the $\bar{N}N$ bound system, the phase volume decreases and the width of the level has to become smaller. This behaviour cannot be obtained in OM whereas it is automatically reproduced in the CCM approach [5].

We finally conclude from Figure 5 the absence of any narrow bound state for this particular optical model. The narrowest one is the first radially excited $^{13}P_0$ state. It has a width $\Gamma$ = 600 MeV.

Nevertheless, even with a big annihilation potential it is possible to obtain states with relatively small width. Such a situation will appear for states located very close to the threshold and being radially excited states. These states have a radius larger than the annihilation range in the KW model and therefore the annihilation potential has no significant influence on them. The same situation is possible for resonant states, as will be shown in the following.

## Resonances

In order to find the near-threshold resonances as well as to understand their physical origin we start by looking into the near-threshold bound state spectra for the OBEP ($W_0$ = 0) in the vicinity of the actual KW cut-off radius ($r_c$ = 1 fm). With decreasing value of $r_c$, the strength of the potential is increased and the near-threshold resonances in the KW model will first appear as bound states. Results are shown in Figure 7. We see the existence of several bound states ($^{11}P_1$, $^{33}P_1$, $^{13}PF_2$, $^{13}P_0$) for $r_c$ values slightly smaller than 1 fm. They are respectively ground ($^{11}P_1$, $^{33}P_1$), first ($^{13}PF_2$) and second ($^{13}P_0$) excited states, as can be seen from Figure 5, and they will manifest as resonances in the KW model. Hereafter we will study their evolution in the Im k < 0 half plane as a function of $r_c$ and $W_0$ as well as their influence on the scattering cross sections.

Let us first consider in Figure 8 the $^{13}P_0$ partial wave. Starting from a bound state in the imaginary axis ($r_c$ = 0.90 fm, E = - 1.75 MeV), this state goes to a resonance region. The symmetric curves in the lower half K-plane correspond to the motion of resonance without annihilation as a function of $r_c$ (i.e. the potential strength). For $r_c$ = 1 the pole coordinates are $k_0$ = (66 - 57i) MeV/c and the position and the width of the resonance obtained from equation (15) are $E_0$ = 8 MeV, $\Gamma$ = 20 MeV.

When we switch on the annihilation potential and keep constant $r_c = 1$ we see that the poles become asymmetrical. Their asymmetry is small because annihilation has small influence on the wave function of this quasinuclear state due to the reasons discussed above. Now the pole coordinates in the K-plane are $k'_0 = (-82 - 76i)$ MeV/c, $k_0 = (46 - 54i)$ MeV/c. Close values for a position of the right pole in the $^{13}P_0$ partial wave for the Dover-Richard and Paris potentials were obtained by a fitting procedure in [14]. However in this work, authors did not determine the position of the left pole.

When annihilation is switched on, the right-left symmetry is broken and the denominator in equation (13) as a function of energy cannot be written in the Breit-Wigner form. Instead of it we have

$$S \sim \frac{1}{(E - E_0(k)) + i\frac{\Gamma(k)}{2}}, \tag{20}$$

where not only the width $\Gamma$, as usual, but also the position of the resonance $E_0$ are functions of the momentum k:

$$ME_0(k) = (k_2k'_2 - k_1k'_1) + (k_1 + k'_1)k \tag{21}$$

$$M\Gamma(k) = 2(k_1k'_2 + k'_1k_2) - 2(k_2 + k'_2)k \tag{22}$$

with $k_0 = k_1 + ik_2$ and $k'_0 = k'_1 + ik'_2$.

These functions, for the $^{13}P_0$ partial wave, are shown in Figure 9a , where the importance of the k-dependence for both $E_0$ and $\Gamma$ is clearly seen.

Because of that, the energy dependence of amplitudes and cross sections, even if they are calculated taking into account only the contribution of isolated poles, will not exhibit the usual maximum at some definite positive energy $E_0$. Instead of it, the near-threshold poles will manifest themselves first of all by a rapid decreasing of

the reduced amplitudes and cross sections with growing k. As can be seen in figure 9b, such behaviour takes place starting from energies very close to the threshold.

An example of asymmetry of the poles' position ($k_0$, $k_0'$) is given by the partial wave $^{33}P_1$ (Fig. 10). In this case the influence of annihilation is dramatic. The left pole lies at positive energy on the physical sheet, but the corresponding wave function has exponentially decreasing asymptotic behaviour as for a bound state.

The main conclusion from these direct calculations of the poles' position, as well as from the fitting procedure performed in [14], is the statement that it is impossible to explain the success of OM in describing the experimental $\bar{p}p$ cross sections at low energy without the existence of near-threshold $\bar{N}N$ P-states. It is also clear from Figure 8 that these levels are created by the nuclear forces, i.e. that they are of quasinuclear nature.

## 5. CONCLUSION

It follows from the results presented in this paper that the physical reason for the enormous P-wave contribution to the $\bar{p}p$ interaction is the same for both the OM and CCM approaches. This reason is the strong attraction between $\bar{N}$ and N due to nuclear-type forces (OBEP). These forces create near-threshold singularities in the $\bar{p}p$ amplitudes, i.e. poles corresponding to the quasinuclear bound and resonant states of the $\bar{N}N$ system. As was shown, annihilation does not destroy these near-threshold states in any case because the radius of such a system is significantly larger than the annihilation range.

At the same time, it is necessary to mention a principal difference between the OM and CCM approaches. Firstly, as was shown here, OM produces states which have no physical interpretation. Further, there is a substantial difference between OM and CCM wave functions inside the interaction region. This fact may be

important, for instance, for understanding the nature of the P-wave dominance effect observed in the reaction $\bar{p}p \rightarrow \bar{\Lambda}\Lambda$ just near the threshold (at relative $\bar{\Lambda}\Lambda$ momenta of few tens MeV/c). This transition is likely to be produced by K and K* exchanges, so that it takes place inside the region of baryon-antibaryon annihilation for the KW model. Wave functions at these distances are strongly suppressed due to absorption, especially in the case of S-states ($|\Psi_S(W_0; r = 0)|^2$ tends to zero faster than $1/W_0$ when $W_0 \rightarrow \infty$, see ref. [5]). Therefore, as was claimed in ref. [13], the relatively large P-wave contribution to the cross section for this production reaction would be caused rather by annihilation than by the attractive nuclear baryon-antibaryon forces. We would like to emphasize that the situation in the CCM is quite opposite. Due to reannihilation $\Psi$ does not tend to zero even at infinitely large values of the constant $\lambda$ defining the coupling between fermion (NN) and meson channels [5].

The dependence of the annihilation cross section $\sigma_a$ on the annihilation constant in the Hamiltonian is also quite different in OM and CCM. In the OM $\sigma_a$ grows with $W_0$ up to the unitary limit, whereas for the simplest version of CCM (for instance, with separable transition potential), we may even have $\sigma_a(\lambda \rightarrow \infty) \rightarrow 0$ because of reannihilation. It is easy to show the latter statement analytically.

Let us introduce the annihilation amplitude $\lambda\mathbb{A}$ calculated in the first order of $\lambda$, but with full accounting of the nuclear forces. So the full annihilation amplitude, $f_a$, will be the solution of the integral equation:

$$f_a = \lambda\mathbb{A} + \lambda^2 \mathbb{A}\, D_0\, \mathbb{A}\, G_0\, f_a, \tag{23}$$

where $D_0$ and $G_0$ are the Green functions of free mesons and fermions correspondingly. Hence,

$$f_a = \lambda(1 - \lambda^2 \mathbb{A}\, D_0\, \mathbb{A}\, G_0)^{-1}\, \mathbb{A} \tag{24}$$

At the same time, for the scattering amplitude induced by reannihilation, $f_{ra}$, we have:

$$f_{ra} = \lambda^2(1 - \lambda^2 \mathbb{A}\, D_0\, \mathbb{A}\, G_0)^{-1}\, \mathbb{A}\, D_0\, \mathbb{A}. \qquad (25)$$

If $f_{ra}$ has no poles (i.e. the reannihilation does not produce bound or resonant states) then at $\lambda >> 1$ we obtain that $f_a \sim \lambda^{-1}$ and $f_{ra} \sim$ const. (on $\lambda$).

For realistic CCM, $f_{ra}$ does have poles (because the reannihilation forces appear to be attractive). This phenomenon creates the oscillation of $f_a$ with increasing $\lambda$, as can be seen from eq. (25) and as was first explicitly demonstrated in [5]. It is necessary to note that, of course in contrast to the quasinuclear states, the reannihilation poles cannot be considered as having a real physical status because their positions and even existence depend on the details of the annihilation mechanism which cannot be taken into account at the present state of our knowledge.

We introduced the above comments on the relations between OM and CCM to emphasize the physical difference of the two approaches. But the main conclusion of this work was formulated in the beginning of this section: the P-wave enhancement effect observed in the low energy $\bar{p}p$ collisions is a manifestation of the quasinuclear near-threshold P-states appearing in any known realistic model of $\bar{N}N$ interaction.

ACKNOWLEDGEMENTS

The authors would like to thank C. Gignoux and R. Moussalam for helpful discussions.

REFERENCES


1. Brueckner W. et al., Phys. Lett.**166B** (1986) 113.

2. Brueckner W. et al., Phys. Lett.**169B** (1986) 302.

3. Batty C.J., Rep. Progr. Phys., **52** (1989) 1165.

4. Brueckner W. et al., Phys. Lett. **158B** (1985) 180;
Linssen L. et al., Nucl. Phys.**A469** (1987) 726.

5. Dalkarov O.D., Protasov K.V. and Shapiro I.S., Int. J. Mod. Phys. **A5** (1990) 2155.

6. Dalkarov O.D. and Myhrer F., Nuovo Cimento **40A** (1977) 152.

7. Bryan R.A. and Phillips.R.J.N., Nucl. Phys. **B5** (1968) 201.

8. Maruyama M. and Ueda T., Nucl Phys. **A364** (1981) 297.

9. Shapiro I.S., Nucl. Phys. **A478** (1988) 665c;
Proceedings of the IV LEAR Workshop, Villars-sur-Ollon, 1987, p. 377.

10. Shapiro I.S., Nucl. Phys. **B8** (Suppl.) (1989) 100;
Antiproton-Nucleon and Antiproton-Nucleus, Ettore Majorana International Sciences Series, V. 47, p. 81.

11. Carbonell J., Dalkarov O.D. and Protasov. K.V., Yad. Fiz. **52** (1990) 1670
[Sov. J. of Nucl. Phys.]

12. Dover C.B. and Richard J.M., Phys. Rev. **C21** (1980) 1466

13. Kohno M. and Weise.W., Nucl. Phys.**A454** (1986) 429; **A479** (1989) 433c.

14. Lacombe M., Loiseau B., Moussalam R. and Vinh Mau R., Phys. Rev. **C29** (1984) 1800.

15. Ueda T., Progr. Theor. Phys. **62** (1979) 1670; **63** (1980) 195.

16. Carbonell J. ,Ihle G. and Richard J.M., Z. Phys. A - Atomic Nuclei, **334** (1989) 329.

17. Bogdanova L., Markushin V.E. and Shapiro I.S., Sov. J. Nucl. Phys. **30** (1979) 248

18. Gal A., Toker G. and Alexander Y., Ann. Phys. **137** (1981) 341.

19. Morimatsu O. and Yazaki K., Nucl. Phys. **A435** (1985) 727.

20. Buck W.W., Dover C.B. and Richard J.M., Ann. of Phys. **121** (1979) 47.

21. Landau R.H. and Schnick J., Phys. Rev. **C36** (1987) 1942.

FIGURE CAPTIONS

Fig. 1. Argand diagram for the partial wave $^{13}P_0$ in the different potentials: solid line - Kohno-Weise model (present calculations); dashed line - Paris potential; dashed-dotted line - Dover-Richard potential (calculations from ref. [14]). Kinetic energy in the $\bar{N}N$ system is presented by triangles (5 MeV), squares (20 MeV) and circles (200 MeV).

Fig. 2(a). Reduced elastic cross section (see eq. (6)) for different partial P-waves with isospin T = 0 as a function of momentum k. The same quantity for pure annihilation scattering ($V_{OBEP}$=0) is presented, scaled with a factor $10^3$.

(b). The same as in Fig. 2a for isospin T = 1.

Fig. 3. Reduced annihilation cross section (see eq. (7)) for different partial P-waves as a function of momentum k.

Fig. 4. Momentum plane (K) and two energy sheets of the Riemannian manifold for the one-channel problem. Solid lines represent different trajectories of S-matrix poles (see text).

Fig. 5. Trajectories of the bound state position in the E-plane in the KW potential as a function of the annihilation strength parameter $W_0$ changing from 0 to 1200 MeV.

Fig. 6. Trajectories of the pole positions in the K-plane as a function of $W_0$.

Fig.7. Binding energies of different P-states in the KW potential as a function of $r_c$. The imaginary part is switched off ($W_0$ = 0).

Fig.8. The K-plane positions of the poles for the partial wave $^{13}P_0$ as a function of $r_c$ and $W_0$.

Fig. 9(a). Dependence of a "position of resonance" $E_0$ (solid line) and "width" $\Gamma$ (dashed line) on momentum k for the partial wave $^{13}P_0$.

(b). Value of $[(E - E_0(k))^2 + (\Gamma(k)/2)^2]^{-1}$ for the $E_0$ and $\Gamma$ from Fig. 9a as a function of momentum k.

Fig. 10. The same as in Fig. 8 for the partial wave $^{33}P_1$.

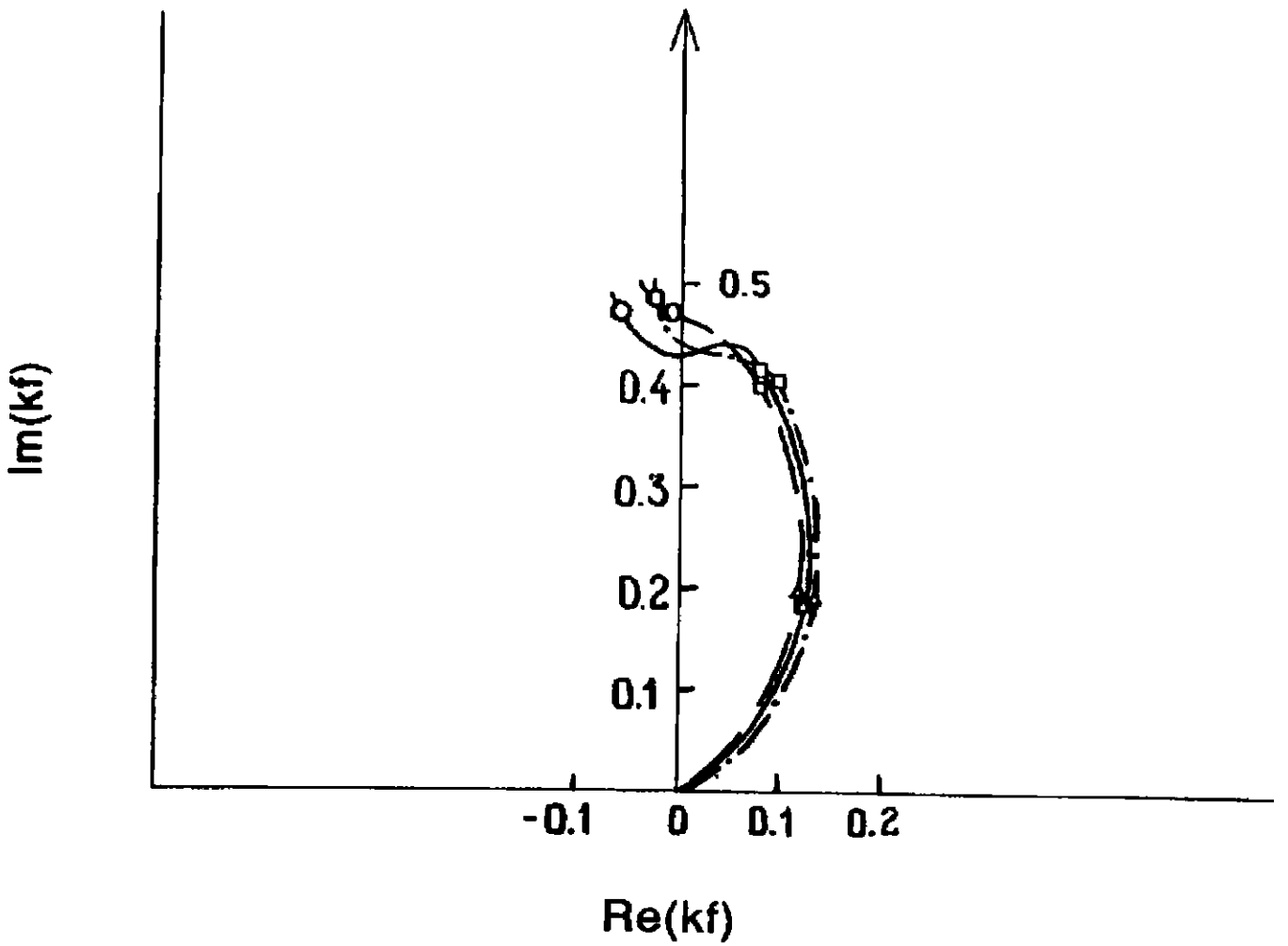


Figure 1

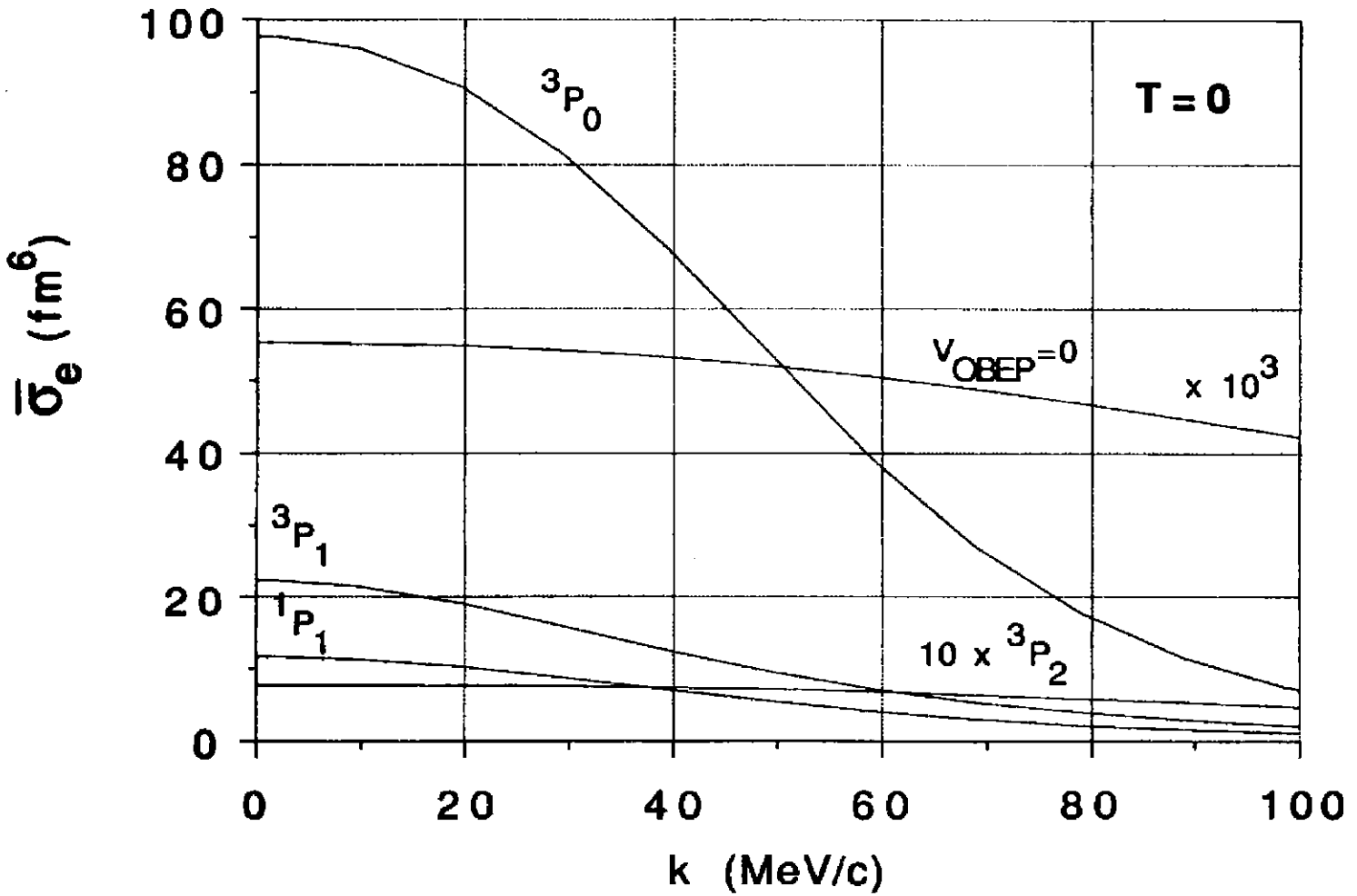
100
80
60
40
20
0
0
20
40
60
80
100
k (MeV/c)
$\bar{\sigma}_e$ (fm$^6$)
T = 0
$^3P_0$
$V_{OBEP}=0$
x $10^3$
$^3P_1$
$^1P_1$
10 x $^3P_2$

Figure 2a

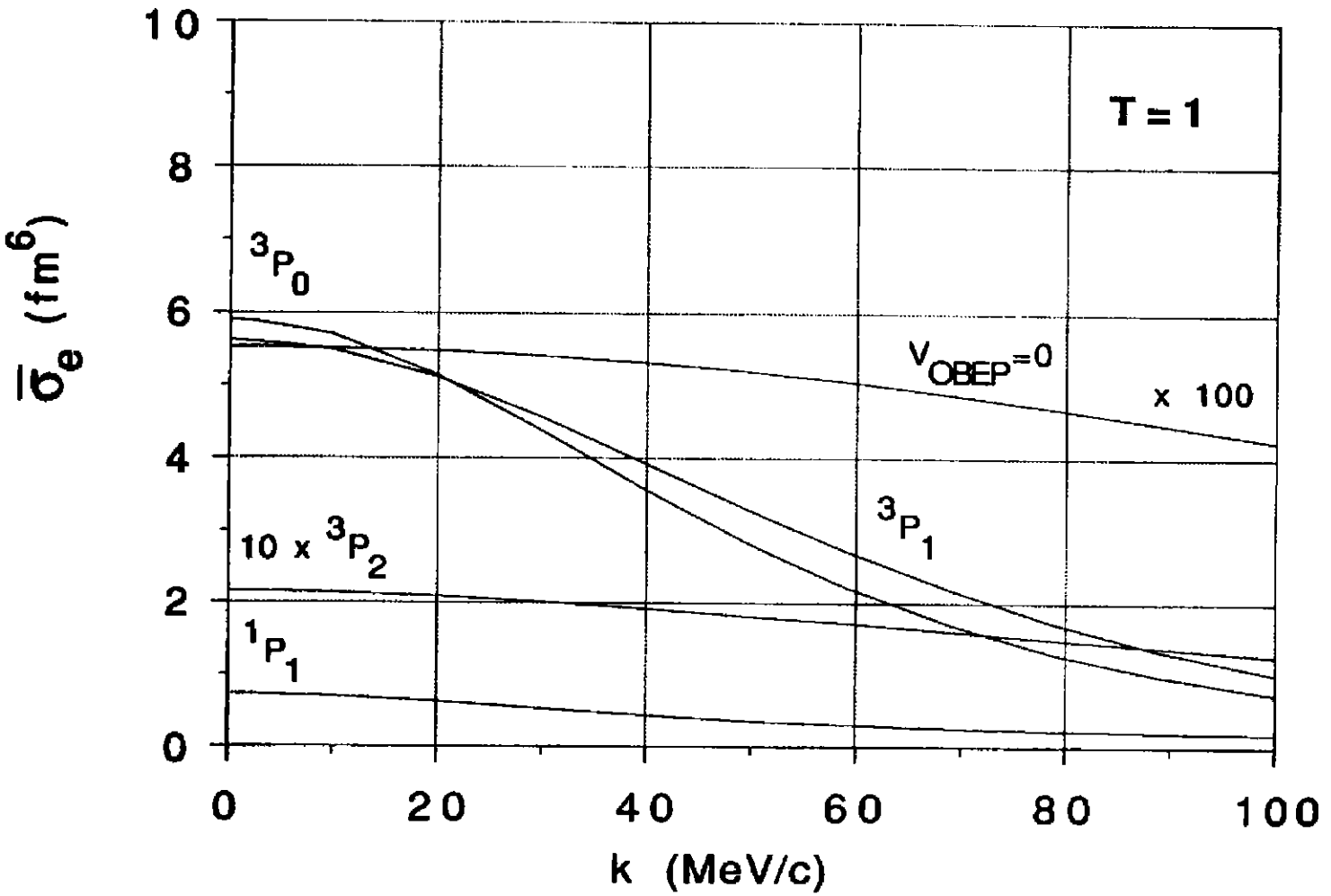
T = 1
$\bar{\sigma}_e$ (fm$^6$)
$^3P_0$
$V_{OBEP}=0$
x 100
$^3P_1$
10 x $^3P_2$
$^1P_1$
0
2
4
6
8
10
0
20
40
60
80
100
k (MeV/c)

Figure 2b

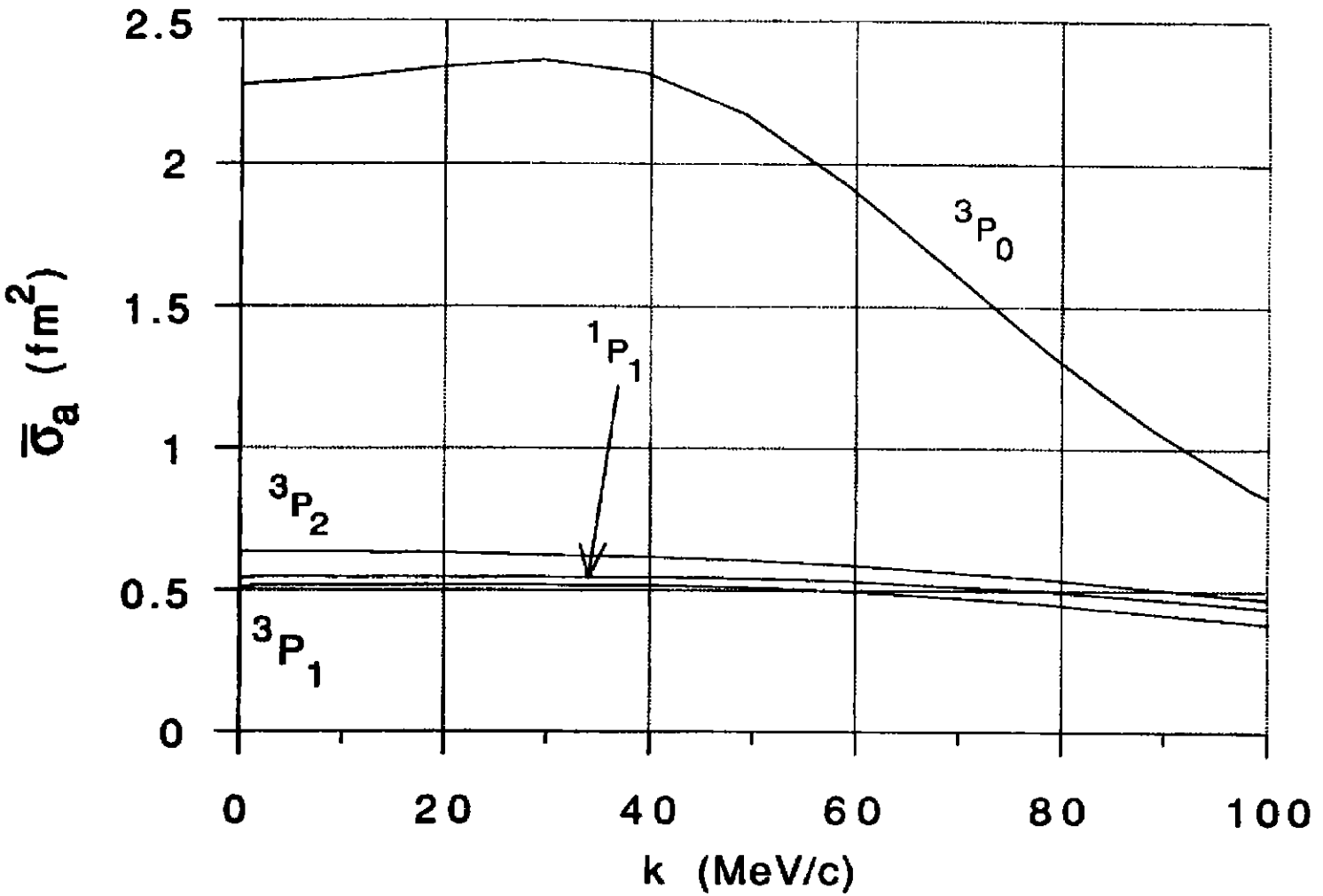
2.5
2
1.5
1
0.5
0
$\bar{\sigma}_a$ (fm$^2$)
$^3P_0$
$^1P_1$
$^3P_2$
$^3P_1$
0
20
40
60
80
100
k (MeV/c)

Figure 3

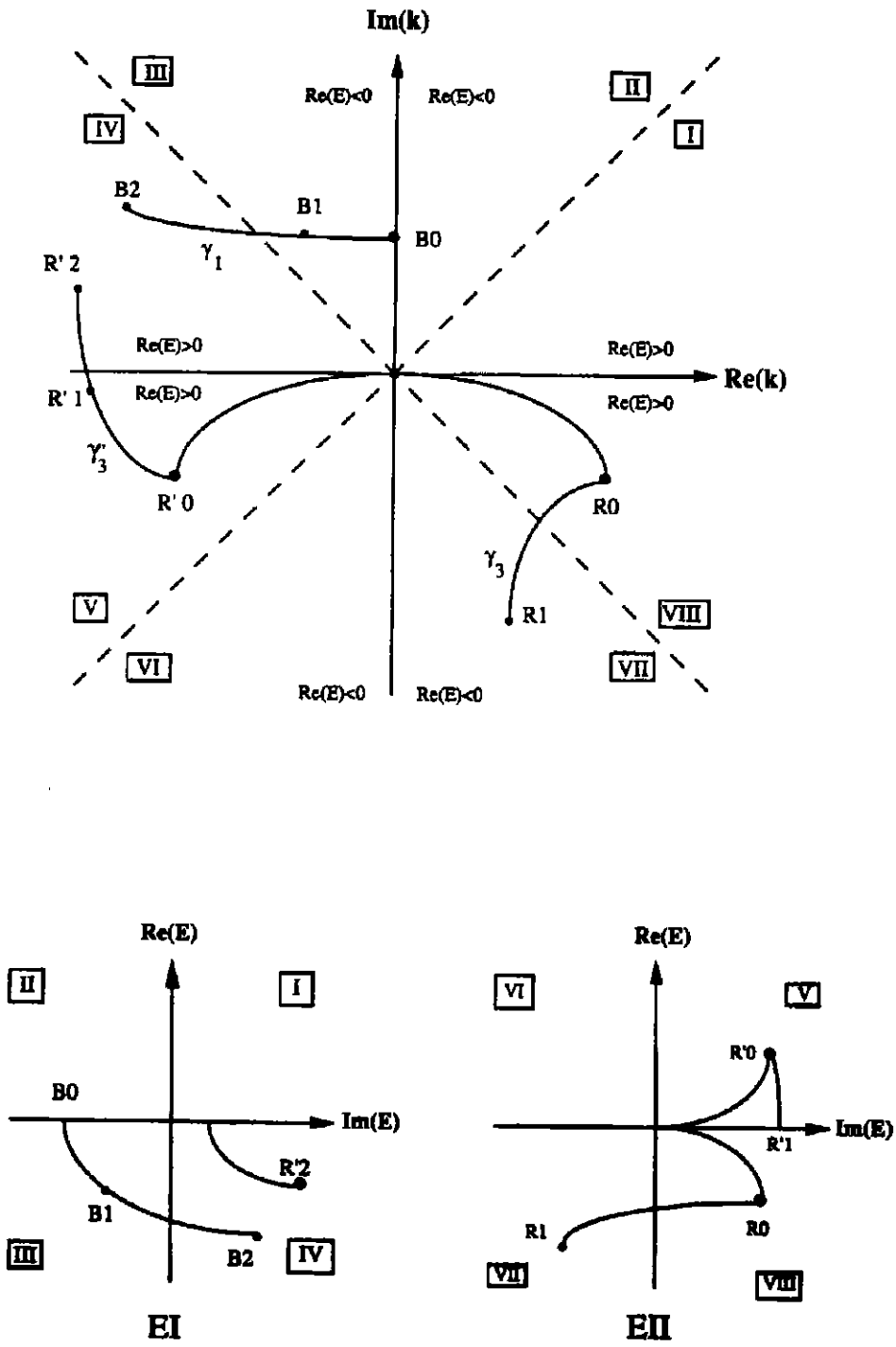
Im(k)
Re(k)
Re(E)<0
Re(E)>0
I
II
III
IV
V
VI
VII
VIII
B0
B1
B2
R0
R1
R'0
R'1
R'2
γ1
γ3
γ'3
Re(E)
Im(E)
EI
EII

Figure 4

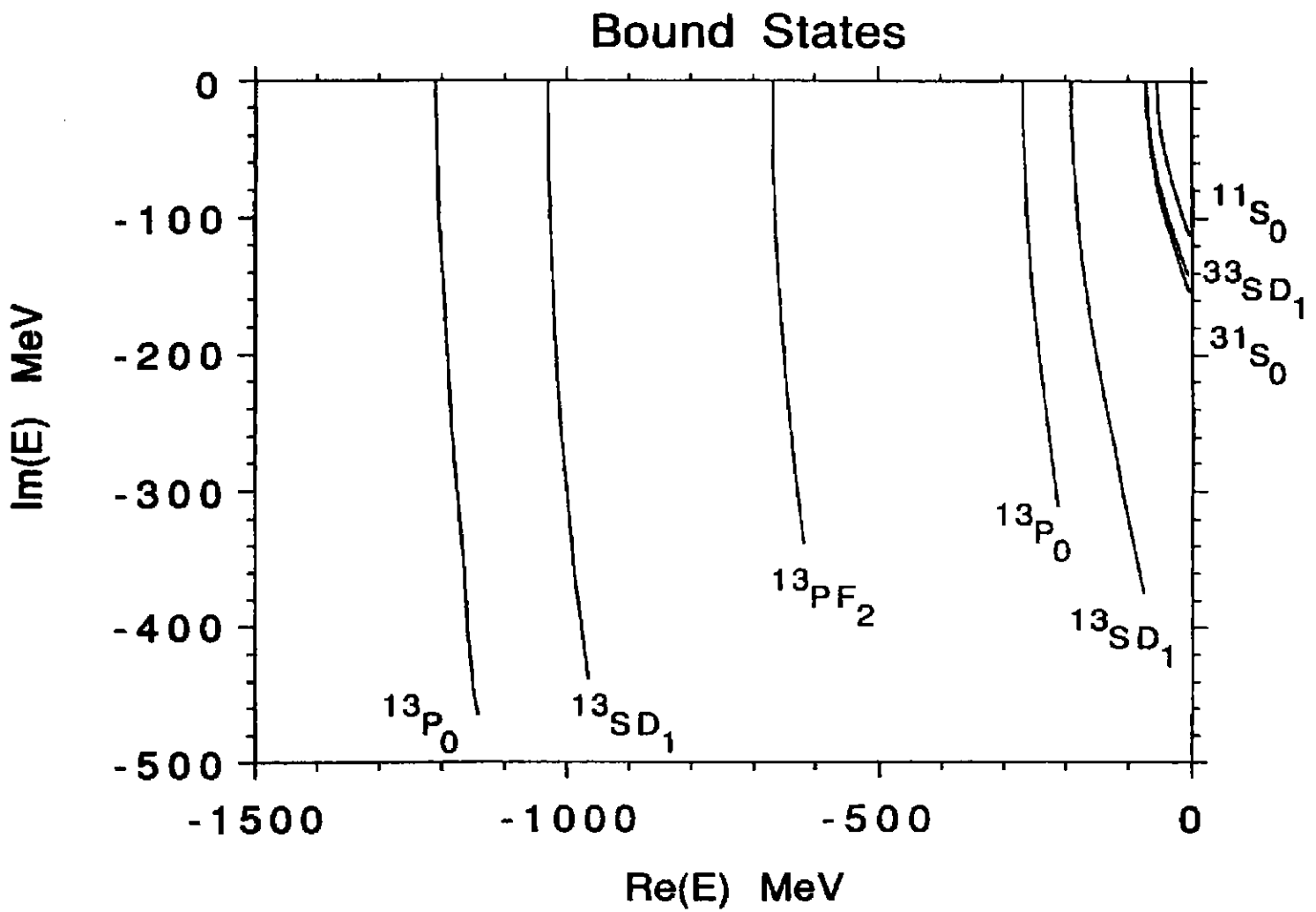
Bound States
0
-100
-200
-300
-400
-500
Im(E) MeV
-1500
-1000
-500
0
Re(E) MeV
$^{13}P_0$
$^{13}SD_1$
$^{13}PF_2$
$^{13}P_0$
$^{13}SD_1$
$^{11}S_0$
$^{33}SD_1$
$^{31}S_0$

Figure 5

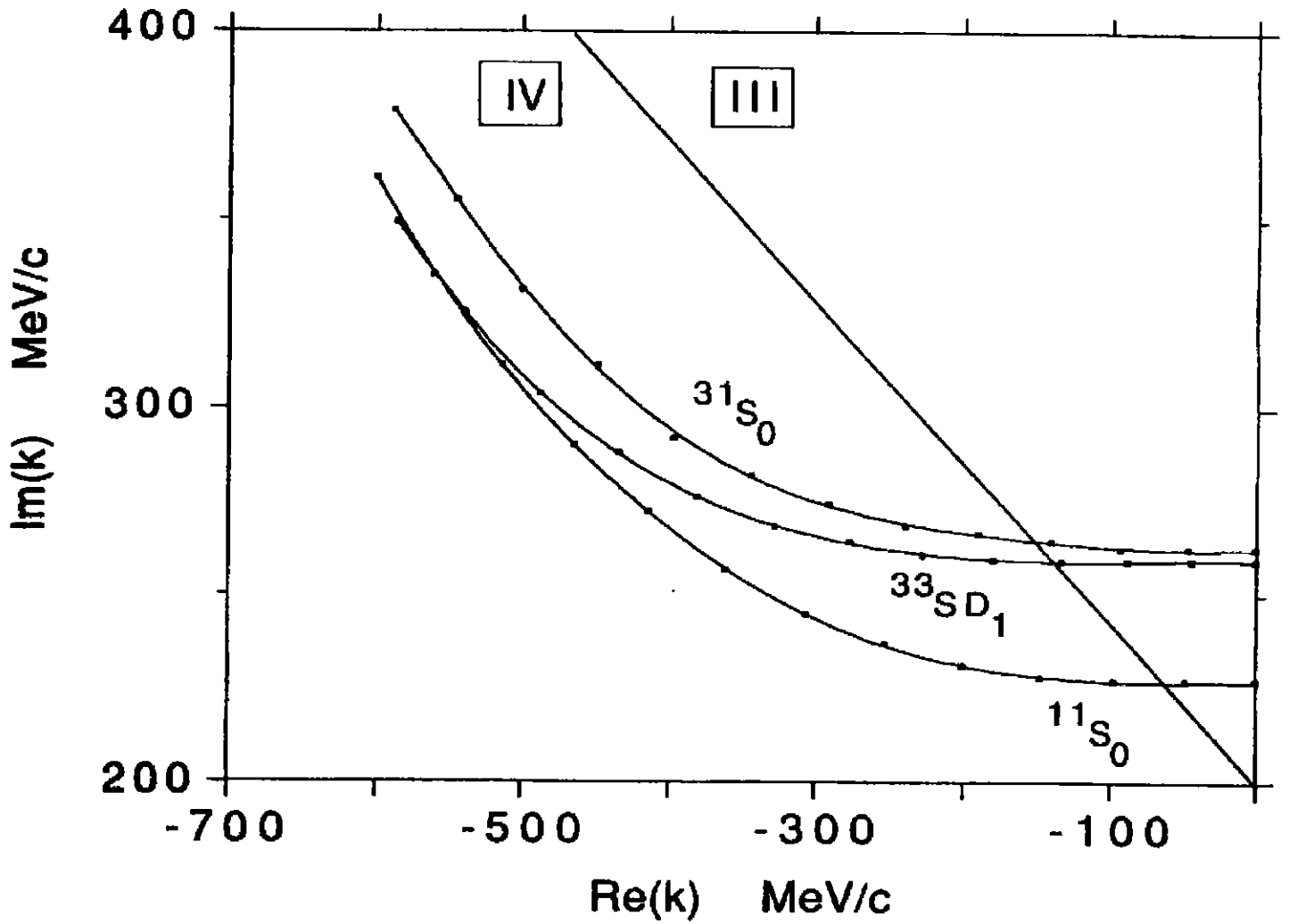
400
300
200
Im(k) MeV/c
IV
III
$^{31}S_0$
$^{33}SD_1$
$^{11}S_0$
-700
-500
-300
-100
Re(k) MeV/c

Figure 6

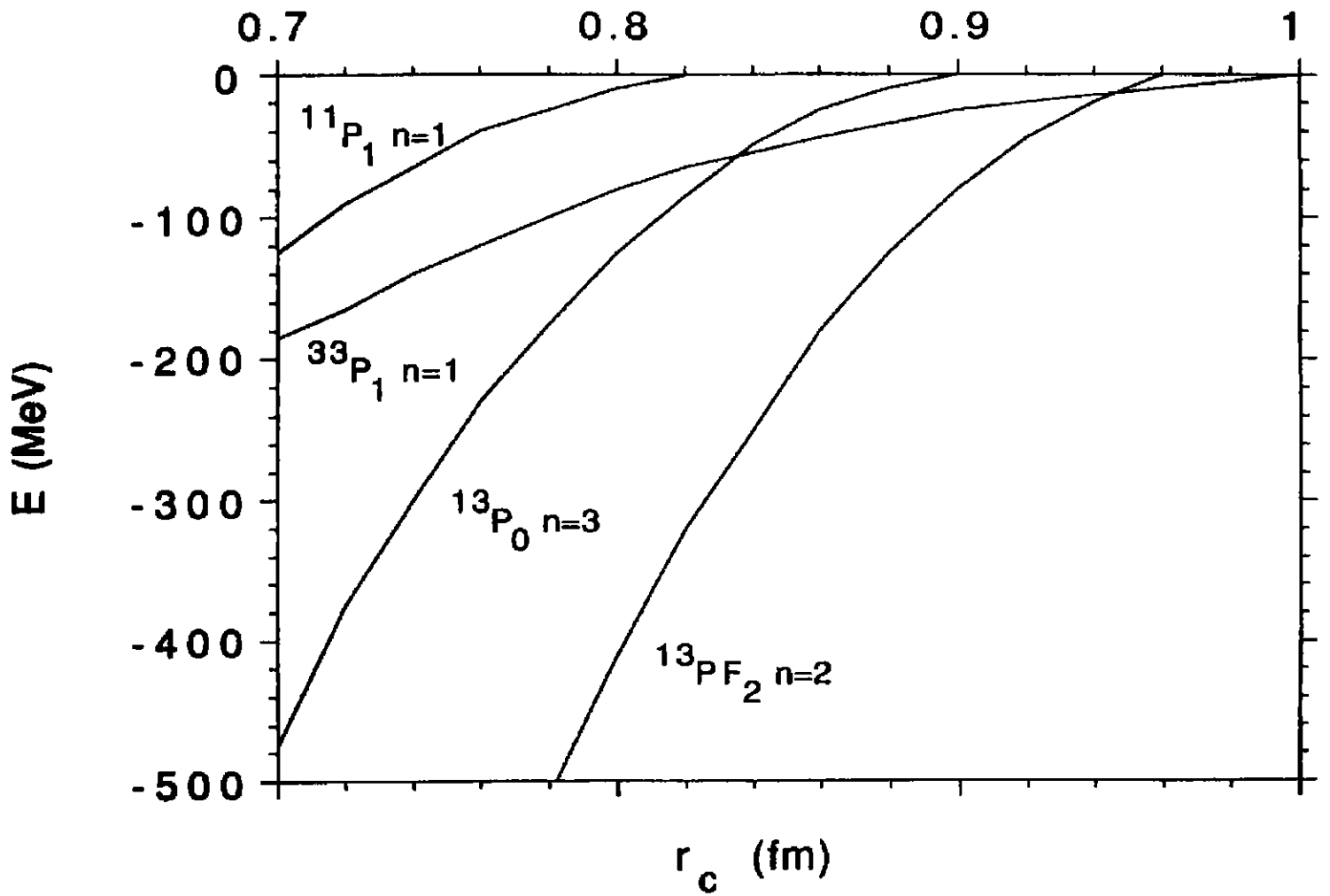
0.7
0.8
0.9
1
0
-100
-200
-300
-400
-500
E (MeV)
$^{11}P_1$ n=1
$^{33}P_1$ n=1
$^{13}P_0$ n=3
$^{13}PF_2$ n=2
$r_c$ (fm)

Figure 7

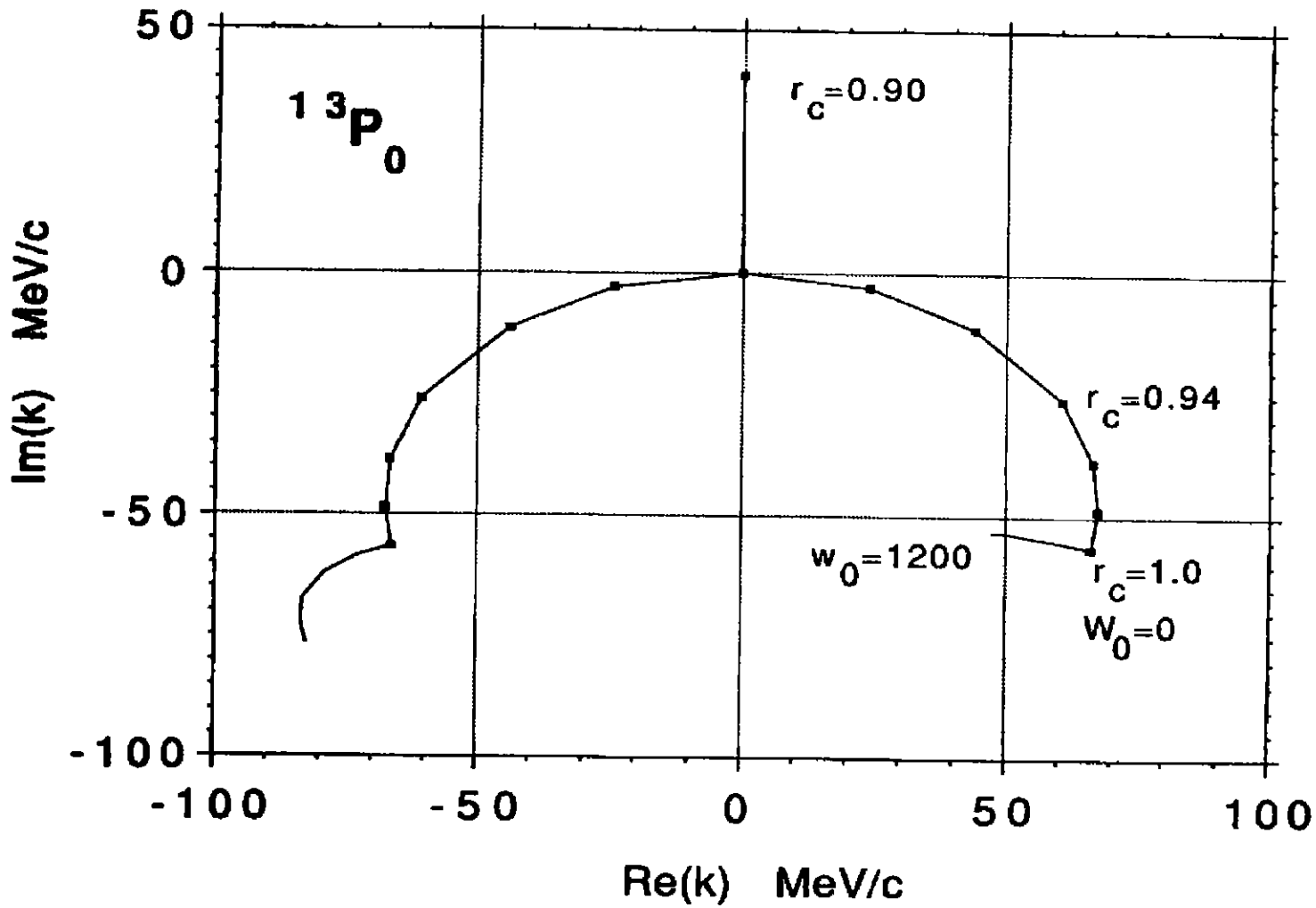
50
0
-50
-100
-100
-50
0
50
100
Im(k) MeV/c
Re(k) MeV/c
$^{1\,3}P_0$
$r_c$=0.90
$r_c$=0.94
$w_0$=1200
$r_c$=1.0
$W_0$=0

Figure 8

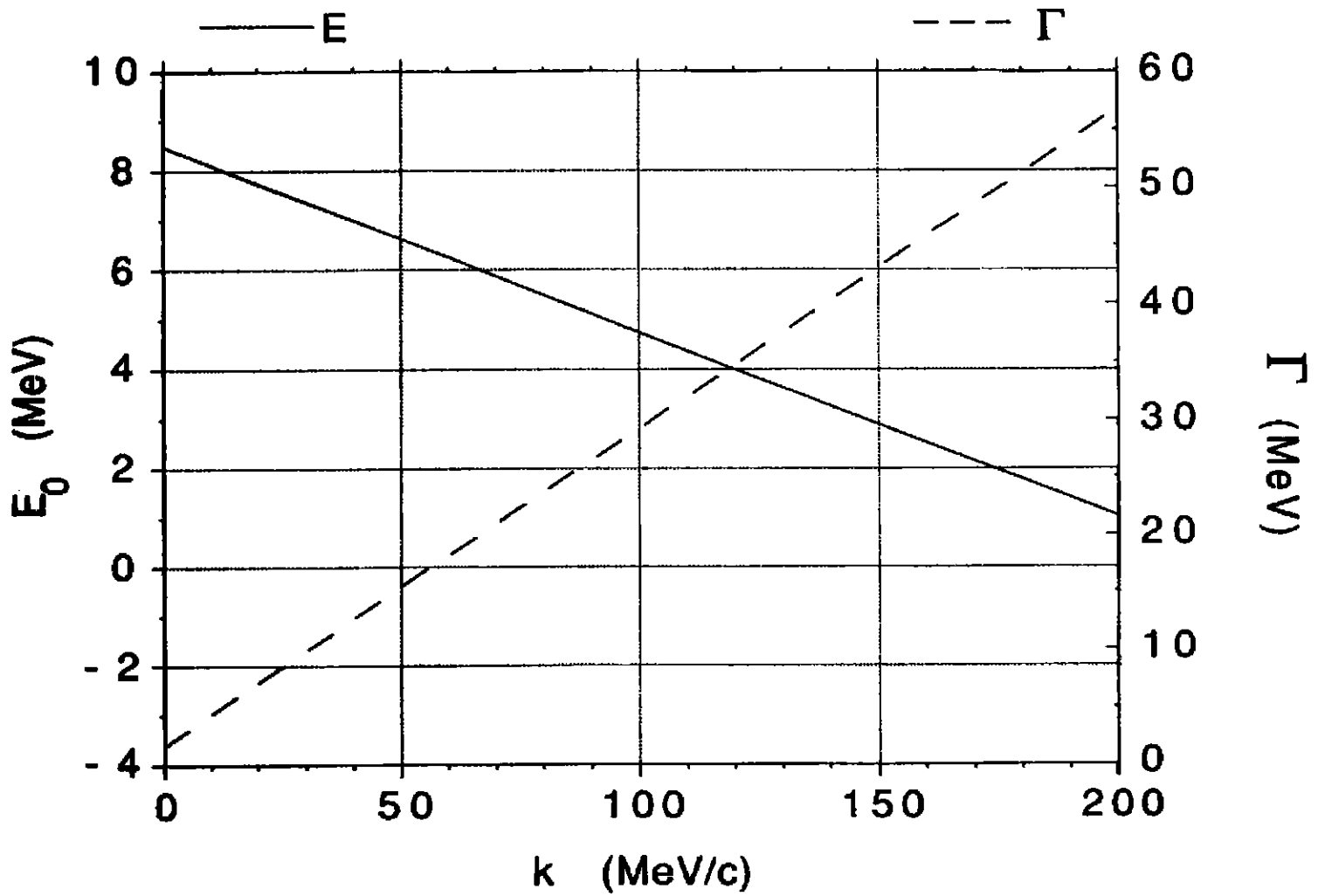
E
Γ
10
8
6
4
2
0
- 2
- 4
$E_0$ (MeV)
60
50
40
30
20
10
0
Γ (MeV)
0
50
100
150
200
k (MeV/c)

Figure 9a

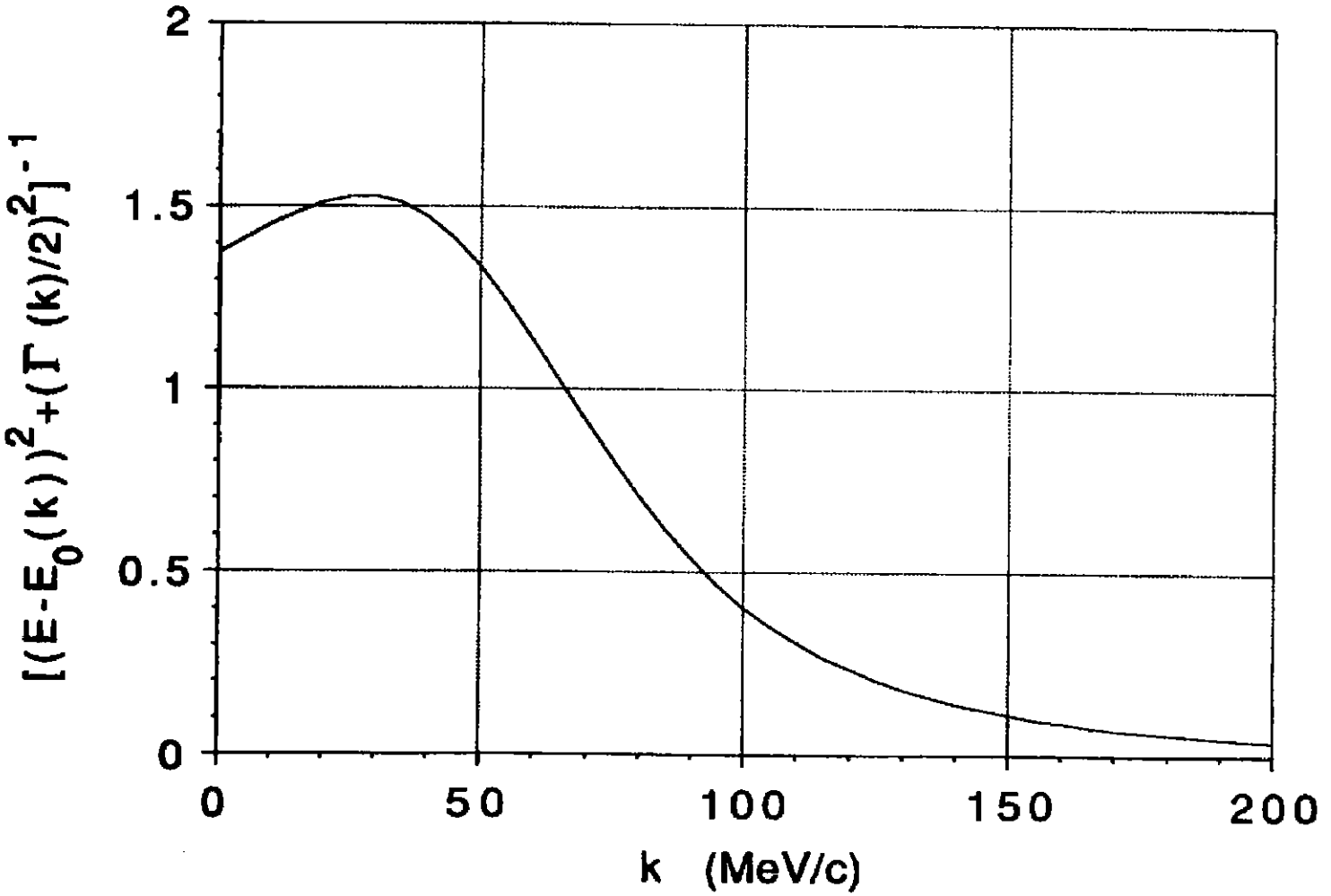


Figure 9b

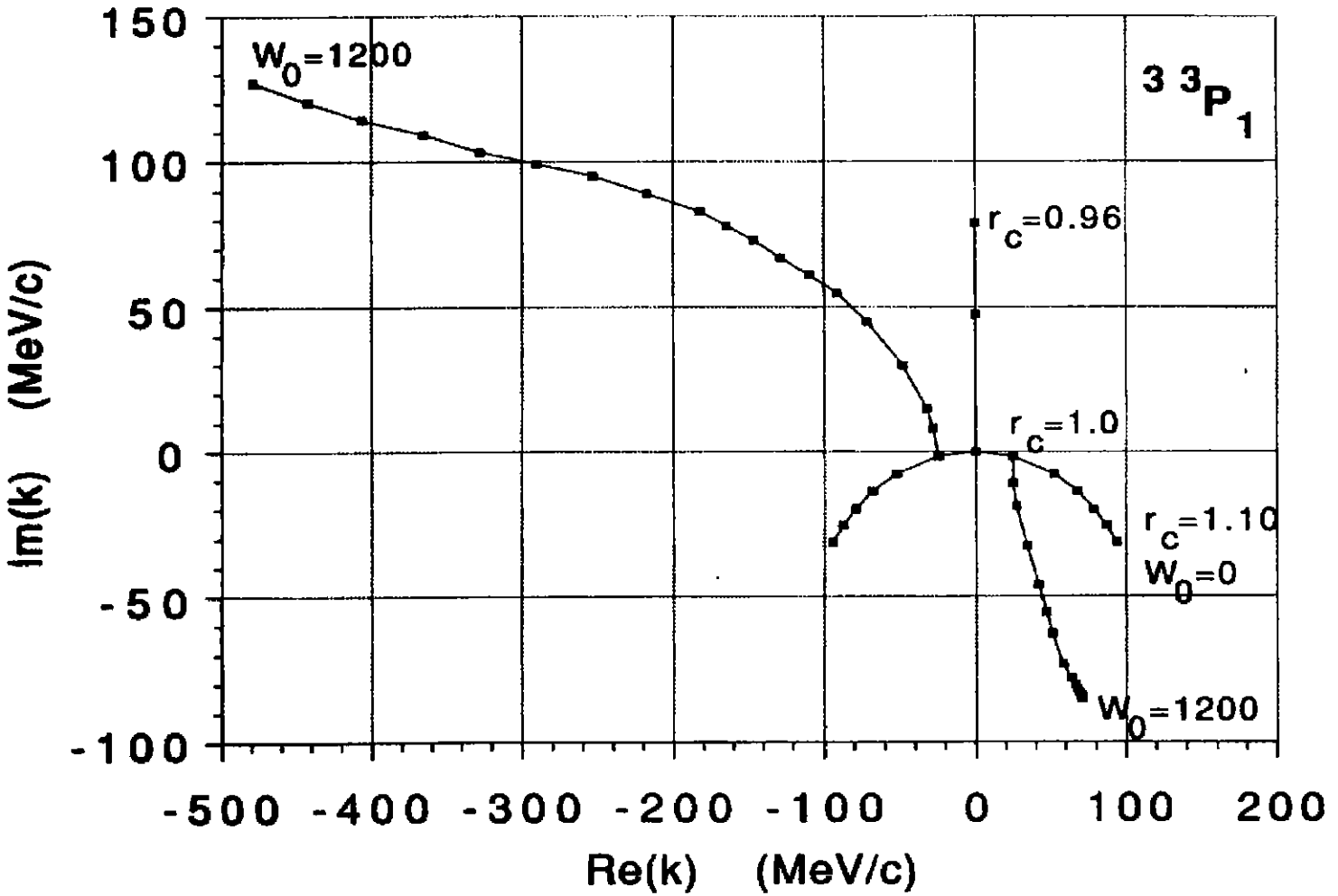
150
100
50
0
-50
-100
Im(k) (MeV/c)
-500 -400 -300 -200 -100 0 100 200
Re(k) (MeV/c)
W0=1200
3 3P1
rc=0.96
rc=1.0
rc=1.10
W0=0
W0=1200

Figure 10